

Resistive ballooning test of the 2DX code

D. A. Baver and J. R. Myra

Lodestar Research Corporation, Boulder Colorado 80301

Maxim Umansky

Lawrence Livermore National Laboratory

1 Introduction

This test was devised to verify the ability of the 2DX eigenvalue code to correctly solve a simple fluid model relevant to edge turbulence in tokamaks. Since the functionality of the 2DX code depends on both the source code itself and the input file defining the system of equations to solve (structure file), this test demonstrates both. Since a similar test was performed on an earlier version of 2DX, this verifies that the current version retains this functionality. Moreover, since the structure file for this test represents a subset of a more general 6-field model, many of the terms in that test are also verified.

This test compares 2DX results to BOUT simulations, and to approximate analytic solutions in the limits of large and small binormal wavenumber.

2 Description

2.1 Code structure

The 2DX code is a highly flexible eigenvalue solver designed for problems relevant to edge physics in toroidal plasma devices. Its flexibility stems from the use of a specialized input file containing instructions on how to set up a particular set of equations. Because of this, the 2DX code permits model equations to be changed without altering its source code. The drawback to this approach is that any change to the structure file represents a potential source of error, necessitating re-verification. This problem is offset by the fact that the source code remains unchanged, thus testing one structure file builds confidence in the underlying code that interprets the structure file. Also, structure files can be translated into analytic form, thus allowing the user to verify that the file contains the equations intended.

The structure file contains two main parts: an elements section, which constructs the differential operators and other functions used in a particular set

of equations, and a formula section, which assembles these into an actual set of equations. This separation means that elements can be recycled in other structure files. By testing one structure file, one builds confidence in the elements used in that file. The main source of error when switching to a different structure file then is in the formula section, which can be manually verified by translating into analytic form.

Regardless of the content of the structure file, the 2DX code is fundamentally a finite-difference eigenvalue solver. As such, it is subject to the limitations of any code of its type.

2.2 Model equations

For this test we use the following model equations [1]-[3]:

$$\gamma \nabla_{\perp}^2 \delta \Phi = + \frac{2B}{n} C_r \delta p - \frac{B^2}{n} \partial_{\parallel} \nabla_{\perp}^2 \delta A \quad (1)$$

$$\gamma \delta n = -\delta v_E \cdot \nabla n \quad (2)$$

$$-\gamma \nabla_{\perp}^2 \delta A = \nu_e \nabla_{\perp}^2 \delta A - \mu n \nabla_{\parallel} \delta \Phi \quad (3)$$

where:

$$\delta p = (T_e + T_i) \delta n + n(\delta T_e + \delta T_i) \quad (4)$$

$$C_r = \mathbf{b} \times \kappa \cdot \nabla = -\kappa_g R B_p \partial_x + i(\kappa_n k_z - \kappa_g k_{\psi}) \quad (5)$$

$$\nabla_{\perp}^2 = -k_z^2 - jB(k_{\psi} - i\partial_x R B_p)(1/jB)(k_{\psi} - iR B_p \partial_x) \quad (6)$$

$$\partial_{\parallel} Q = B \nabla_{\parallel} (Q/B) \quad (7)$$

$$\nabla_{\parallel} = j \partial_y \quad (8)$$

$$\delta v_E \cdot \nabla Q = -i \frac{k_z (R B_p \partial_x Q)}{B} \delta \Phi \quad (9)$$

$$\nu_e = .51 \nu_r n / T_e^{3/2} \quad (10)$$

2.3 Boundary conditions

This test case uses phase-shift periodic boundary conditions in the parallel direction, and zero-derivative boundary conditions in the radial direction. The phase shift in the parallel direction is given by:

$$e^{i2\pi n q} \quad (11)$$

2.4 Profile setup

The formulas in Eq. 1-3 are normalized to Bohm units. Distances are measured in units of ρ_s and time is measured in units of ω_{ci}^{-1} , with ρ_s and ω_{ci} calculated at reference values of n_e , T_e , and B . Profiles of n_e , T_e , and B are provided as multiples of these reference values. Output eigenvalues are multiplied by ω_{ci} . Resistivity is given by the formula:

$$\nu_r = \frac{\mu}{.51\sigma} \quad (12)$$

where

$$\sigma = 1.96 \frac{\omega_{ce}}{\nu_{ei}} \quad (13)$$

The geometry used is an idealized toroidal annulus with major radius R , minor radius a , and thickness δa . The density profile is exponential with scale length L_n , and temperature profiles are flat. Curvature is assumed, and is given by:

$$\kappa_n = \frac{\cos(y)}{R} \quad (14)$$

The function q may be sheared, but shear is set to zero for the test case given. The value of this constant q is given in Sec. 4.

Parallel derivatives are calculated using the Jacobian factor $j = 1/qR$. Toroidal mode number is calculated by $n = k_z a/q_0$.

3 Analytic results

The solutions to the equation set in Eq. 1-3 can be solved by first assuming that $\mu \gg 1$, in which case the equations can be reduced to the form:

$$\partial_y^2 \delta\Phi + \frac{\alpha}{\gamma} (\gamma_0^2 \cos(y) - \gamma^2) \delta\Phi = 0 \quad (15)$$

where:

$$\alpha = \frac{q^2 R^2 k_z^2}{\sigma} \quad (16)$$

$$\gamma_0 = \sqrt{\frac{2}{RL_n}} \quad (17)$$

For the limit where k_z is very large, we can use the approximation $\cos(y) \approx 1 - y^2/2$ to get a Hermite equation. This results in the approximate solution:

$$\gamma = \omega_{ci} \left(\gamma_0 - \frac{\sqrt{\frac{\alpha\gamma_0}{8}}}{\alpha} \right) \quad (18)$$

For the limit where k_z is very small, a more complicated approximation can be used. This arises from the ansatz $\delta\Phi = e^{inq\theta} + Ae^{i\theta(nq+1)}$. This yields the analytic formula:

$$\frac{\alpha^2\gamma_0^4}{2\gamma(1+2nq)} = \alpha\gamma + n^2q^2 \quad (19)$$

4 Numerical results

The code was tested by sweeping the variable k_z from .001 to 1000 cm and plotting the fastest growing eigenvalue. The parameters used in this test are shown in table 1:

$$\begin{aligned} a &= .75 \text{ cm} \\ \delta a &= .3 \text{ cm} \\ R &= 207.5 \text{ cm} \\ L_n &= 9.4 \text{ cm} \\ Z_{eff} &= 32 \\ B &= 1 \text{ T} \\ n_e &= 10^{14} \text{ cm}^{-3} \\ m_i/m_p &= 2 \\ \mu &= 10^4 \\ T_i &= 1 \text{ eV} \\ T_e &= 100 \text{ eV} \\ \ln\Lambda &= 12.4 \end{aligned}$$

The results of this test are shown in Fig. 1. The red lines near the ends of the plot are analytic solutions. The blue dashed line is the asymptotic limit of the analytic solution for high k_z . The green dots are solutions from 2DX, whereas the black dots are solutions from a previous version of 2DX using a 2-field model. The blue crosses are simulation results from BOUT. In addition, a table of the raw eigenvalue data is shown in table 2.

References

- [1] H. Strauss, Phys. Fluids **24**, 2004 (1981).
- [2] T. C. Hender, B. A. Carreras, W. A. Cooper, J. A. Holmes, P. H. Diamond, and P. L. Similon, Phys. Fluids **27**, 1439 (1984).

- [3] P. N. Guzdar and J. F. Drake, *Phys. Fluids B* **5**, 3712 (1993).

nx	4	ny	16
dx	.693242	dy	.392699
γ	$\gamma(s^{-1})/4.79 \times 10^7$	n	.5 $k_z(cm^{-1})$
μ	10^4	ν_r	.00131267
q	1.5	k_z	-.144249 $k_z(cm^{-1})$
j	.000474896	k_ψ	0
κ_n	.00711444 $\cos(y)$	κ_g	0
B	1	RB_p	1
n_0	$e^{-x/65.1647}$	T_e	1

Table 1: Non-dimensional profile functions and parameters used in the resistive ballooning test case, as a function of the dimensional input $k_z(cm^{-1})$.

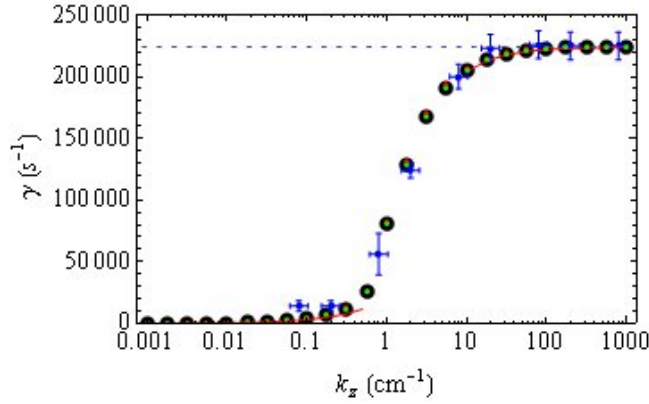


Figure 1: Growth rate vs. k_z for the resistive ballooning model. Green dots are solutions from 2DX, black dots are solutions from 2DX from a 2-field model, blue crosses are BOUT results, and red lines are analytic results.

$k_z(cm^{-1})$	$\gamma(s^{-1})$	$k_z(cm^{-1})$	$\gamma(s^{-1})$
.001	7.65881	1.77283	127813
.00177283	13.7556	3.16228	167064
.00316228	792.258	5.62341	191107
.00562341	3890	10	205355
.01	3812.59	17.7283	213607
.0177283	3880.01	31.6228	218291
.0316228	4026.53	56.2341	220651
.0562341	4431.82	100	221637
.1	5429.65	177.283	222045
.177283	7606.79	316.228	222220
.316228	12267.2	562.341	222284
.562341	24588.4	1000	222305
1	80744.4		

Table 2: Growth rate vs. k_z for the resistive ballooning model.